Volume 67, Issue 4, 2023
Journal of Scientific Research
of
The Banaras Hindu University

Efficacy Analysis of Microwave Assisted Silver and Gold Doped Hydroxyapatite for Orthopedic Applications

'Natarajan N[1*] Prabasheela B[2] and Vijayalakshmi R[3]

[1]Biotechnology &Engg, AVIT, Vinayaka Mission's Research Foundation, Tamil Nādu. naganatarajan@gmail.com.
[2]Biotechnology&Engg, AVIT, Vinayaka Mission's Research Foundation, Tamil Nadu. prabasheela@avit. ac. in
[3]PG & Research Department of Zoology, A.D.M.C, Bharathidasan University, Tiruchirappalli.
Tamilnadu.vijayarvenkat@gmail.com

Abstract: **Using an improved microwave process, hydroxyapatite (HAP), silver-doped hydroxyapatite (HAP-Ag), and gold-doped hydroxyapatite (HAP-Au) were produced and designated as A1, A2, and A3, respectively. Through studies on cell proliferation and antimicrobial agents, this research focuses on the synthesis, characterization, and application standpoint. X-ray diffraction, Fourier-transform infrared (FT-IR), Raman spectroscopy, and scanning electron microscopy (SEM) were used to characterize the A1, A2, and A3 composite's morphology and structure. The biocompatibility investigations were conducted utilizing accepted techniques like Zone of Inhibition, which included pathogenic bacteria and fungus. Fibroblast cell lines were used in the cell compatibility studies to better understand the cell multiplication within the allotted time frame. The synthetic composites fared better in terms of bacterial suppression and showed excellent matrix characteristics and cell proliferation. The structural changes are visible as the A2 has shown predominant character towards the zone of inhibition when compared with the other groups. Additionally, a homogeneous distribution of the Ag and Au on the HAP structure was observed through SEM. Some of the miscellaneous challenges will be further evaluated in the subsequent studies.**

Index Terms: **Antibacterial and fungal, Bio-compatibility Cell toxicity, Hydroxyapatite, Microwave method, Tri-Calcium Phosphate.**

I.INTRODUCTION

One family of materials called bio-ceramics is utilized to replace or repair damaged bone tissue. It can directly interact with surrounding tissue, either stimulating new tissue regeneration or supporting tissue growth, depending on the application. Bio-ceramics serve a multitude of purposes in the restoration of biological processes like osteo-induction and osteo-regeneration. They can be produced chemically or by arising in different forms and phases. Hydroxyapatite (HAP) is an aesthetically pleasing inorganic bio-ceramic material. The microstructure of bio-ceramics composition (stoichiometry or purity), homogeneity, phase distribution, morphology, grain size/grain shape, grain boundaries, crystalline size, crystallinity, pores, cracks, and surface, etc. When designed appropriately, its crystalline structure, chemical makeup, and particle shape can replicate the physical and chemical characteristics of the human teeth and bone's inorganic components (Olszta et al., 2007, Dey et al., 2010).

The osteoblast matrix created by HAP crystals in the body forms bones (Santos et al., 2008, Tang et al., 2009, Ren et al., 2009, Petit, 1999,

DOI: 10.37398/JSR.2023.670412

Ramesh, 2001, Sinha et al., 2009, Mishra 2009, Coreia et al., 1996, Best et al., 2008, Dubok, 2000). Numerous bio-applications, such as immunological sensing (Hench, 1991), bone-tissue regeneration (Turkoz et al., 2017: Suganya et al., 2017: Balakrishnan et al., 2017), and hemocompatibility enhancement (Gupta Y. et al., 2006), have reported on the remarkable capabilities of HAP composites. Sebastiammal S. et al. (2022)successfully synthesized and physico-chemically characterized HAP doped with silver(Ag) nanoparticles, and found enhanced antibacterial activity. Because HAP has several vacancies in its chemical structure that allow for the acceptance of nanoparticles like silver and gold. It is a promising candidate for developing a hybrid molecule. Consequently, researchers are concentrating on utilizing silver to create novel bioactive chemicals at the nanoscale. There are reports in the literature suggesting that electrostatic attraction between negatively charged bacterial cells and positively charged nanoparticles is critical for nanoparticle activity as bactericidal materials, even though the exact mechanism of Ag nanoparticles' antibacterial action is unknown (Dubok 2000, Hench 1991). The increased antibacterial activity of a synthesized HAP composite including collagen (alginate) was reported by Serhiienko, A. (2021).

Several mechanisms have been proposed that involve silver interacting with biological macromolecules (Ding et al,2007) such as enzymes and DNA via an electron-release mechanism (Gupta et al,2006). When exposed to Ag+, DNA is thought to lose its replication ability, and cellular proteins are inactivated (Arumugam et al,2006). Furthermore, it has been demonstrated that Ag+ binds to functional groups of proteins, resulting in protein denaturation [Hickmaen 2015]. Silver ions were embedded in bio-properties materials to achieve high biocompatibility and optimal antibacterial properties in the new compounds (Hulbert et al,1987]. On the other hand, Nishat Arshi et al.(2011) reported the antibacterial activity of gold nanoparticles as a function of particle concentration against the gram-negative bacterium *Escherichia coli (E. coli)* was tested in solid growth media. The two types of gold nanoparticles exhibit strong antibacterial activity, with a zone of inhibition of approximately 22 mm against *E. coli* (ATCC 25922 strain). Even though silver nanoparticles have antibacterial activity against many organisms, there are some limitations, gold nanoparticles have a dual role of strong compatibility with human tissues and some extend to biocidal activity.

To improve the production process for HAP-doped silver and gold nanoparticles, a comprehensive characterization and demonstration of the current advanced microwave approach (Natarajan N. 2018) is provided. The structure, morphology, and optical characteristics of highly crystalline nanopowders of HAP, HAP-Ag, and HAP-Au were examined using X-ray diffraction (XRD), Fourier transform infrared (FT-IR), Raman spectroscopy, and scanning electron microscopy(SEM). Gram-positive and negative organisms illustrate the fungus family's biocompatibility and antibacterial qualities. The most encouraging aspect of the synthesized HAP composites was revealed by the considerable vitality of cell growth employing fibroblast cell lines throughout the research.

II.MATERIAL AND METHODS

The synthesis of A1(HAP), A2(HAP-Ag), and A3(HAP-Au) involved the use of di-hydrogen ammonium phosphate and calcium hydroxide in molar ratios of 1 M and 0.6 M, respectively, as a precursor to accomplish the 1:6 ca & phosphate reaction in the final composition with the application of sophisticated microwave method. Here are the specifics:

A. *Synthesis of Hydroxyapatite(A1) using the Microwave method*

The HAP was synthesized in a controlled environment at an operating temperature of 45 °C using IRTECH brand Advanced Microwave technology. By adding diluted colloidal alkali, the pH of the solution is kept at alkali, allowing the reaction to remain between 10 and 11. After the calcium hydroxide's hydroxyl group (OH^-) was liberated, it interacted with the phosphate sources to create hydroxyapatite [$Ca_{10}(PO_4)_6(OH)_2$] from the di-ammonium hydrogen orthophosphate. The synthetic powder was left to age for a minimum of eight hours. Following the aging process, the precipitates underwent two or three washings to reduce the pH to almost 7.0. To perform phase transfer to TCP, Tri-calcium phosphate-TCP, or Bi-calcium phosphate B, the dry powder was finely ground and then calcined at various RAMP rates, 2

to 3°C per minute, till 1100 ºC.

B. Synthesis of Silver nanoparticles doped Hydroxyapatite (Ag- Hap) using the Microwave method

HAP-Ag was created by maintaining the same chemical composition, but the components were dispersed in a 10-3 molar solution of silver nitrate rather than de-ionized water, and a few drops of 0.1% sodium borohydride were added to decrease the silver nanoparticles. The white tint was slightly altered to yellow. Subsequently, the entire solution underwent the microwave treatment described in the preceding protocol to create intercalation between the precursors. Following the treatment, a stable purple-colored A2 was generated, and it was aged for 8 hours. The aged A2 doped powder was then calcined in the RAMP described in the previous paragraph.

C. *Synthesis of Gold nanoparticles doped Hydroxyapatite (A3) using the Microwave method*

To create HAP-Au, the same chemical composition was kept, but the components were dissolved in a 10-3 molar solution of chloroauric acid ($HauCl_4$) rather than de-ionized water. To lessen the gold nanoparticles, a few drops of 0.1% sodium borohydride were applied. The hue was somewhat altered turning purple from white. Subsequently, the entire solution underwent the microwave treatment described in the preceding protocol to create intercalation between the precursors. Following the treatment, a stable purple-colored A3 was created, and it was given eight hours to age. Following the aging process, the A3 doped powder will be calcined in the RAMP described in the previous sentence.

Three treatment groups—A1 (hydroxyapatite), A2 (silver nanoparticles doped hydroxyapatite), and A3 (gold nanoparticles doped hydroxyapatite)—were used in this work. They underwent various characterization tests, including FTIR, RAMAN, TGA, SEM with EDAX, and XRD. The antimicrobial and cell proliferation assays demonstrated the biocompatibility of the three treatment groups (A1, A2, and A3).

D. Antibacterial studies

A paste was created by combining 20 mg of the sample with 10µl of sterile distilled water, and it was then placed onto the sterile disc. The test microorganisms utilized for antimicrobial analysis are *Streptococcus mutans, Staphylococcus aureus, Klebsiella pneumoniae*, and *Escherichia coli.* The bacterial strains were maintained alive using nutrient agar (NA). Nutrient agar plates were infected with pure bacterial cultures, which were then cultivated for 24 hours at 37ºC. A bacterial suspension of 1.5x108 cfu/ml was obtained by aseptically mixing the new culture to 2 ml of sterile saline and setting the cell density to 0.5 McFarland turbidity standard. This process created the inoculum. In 1000 ml of distilled water, dissolve 38 grams of Muller Hinton Agar Medium (Hi-Media) to create the medium.

The medium was autoclaved for fifteen minutes at 121°C and fifteen pounds of pressure. After the autoclaved medium had cooled, it was well combined and transferred into petri dishes. (15% per dish). The 100ul bacterial test cultures (*Escherichia coli, Staphylococcus aureus, Klebsiella pneumoniae, and Streptococcus mutans*) were swabbed onto the plates using a sterile L-rod.
Sample Loaded (20 mg) The Muller-Hinton agar medium was then covered with discs, and the plates were incubated for a full day at 37°C. The inhibition zones surrounding the disc were inspected and measured using a transparent ruler after the incubation period. The size of the disc and the zone of inhibition were assessed. It was believed that there was inactivity because there was no zone inhibition (Kohner et al., 1994; Mathabe et al., 2006). According to Assam et al. (2010), the activities are categorized as sensitive if the zone of inhibition is higher than 11 mm, moderate (8–10 mm), and resistant if it is less than 7 mm.

E. Anti-fungal studies by Disc Diffusion Method (Bauer et al., 1966)

Agar disc diffusion (Kirby–Bauer) tests were used to determine antibiotic susceptibility. Fungi strains *Aspergillus flavus, Aspergillus niger, and Candida albicans* were swabbed in Sabouraud Dextrose Agar (SDA) plates with sterile cotton swabs. The Sample (20mg) loaded Discs were then placed on the surface of the SDA medium, and the compound was allowed to diffuse for 5 minutes before the plates were kept at 22°C for 48 hours of incubation. At the end of the incubation period, the

inhibition zones around the disc were examined and measured with a transparent ruler.

F. In vitro cytotoxicity assay (Test on extract (ISO 10993-5)

100 mg of test materials were incubated in 1 ml of MEM at 37°C for 24 hours to prepare the extracts. Diluted phenol is the positive control. In MEM, dilute the stock solution of phenol (13 mg/ml) to 1.3 mg/ml. Ultra-high molecular weight low-density polyethylene was used as the negative control. 30 cm2 of this material was incubated for 48 hours at 37°C in 24 ml of MEM to create the extract. Growing at 37°C in a humidified environment of 5% CO_2/95% O_2, L929 cells were cultured in Modified Eagle medium (MEM, Gibco, Life Technologies, Grand Island, NY) supplemented with 2 mmol/L L-glutamine (Gibco), 100 IU/mL, 100 mg/mL penicillin-streptomycin (Gibco), and 10% foetal bovine serum (Gibco). treated with 0.5 mmol/L EDTA (Gibco) and 0.05 percent trypsin before being gathered in culture media at the confluence. After the cell suspension was seeded into 96-well culture plates at a ratio of 1 104 cells/ml in MEM, it was counted using a Neubauer chamber and allowed to sit at 37°C in 5% CO_2 for 24 hours. Insoluble particles were extracted from the extracts made by the previous process using centrifugation. Next, a 50% extract concentration was obtained by either using the extracts 100% pure or combining them with an equivalent volume of 2x MEM. The medium's pH was raised to 7.4 using sodium bicarbonate. After that, this was diluted with twice as much MEM to get 25% and 12.5%. The sole reagent control that was employed was media. On an L929 cell monolayer that is not yet confluent, There were three controls: a positive control, a negative control, and various dilutions of the test sample extracts. After extracts and controls were incubated at 37°C for 24±2 hours, 10x microscope images were taken, and an MTT assay was performed.

The procedure was as follows: all test and control wells were filled with 30µl of reconstituted MTT solution (15 mg MTT in 3 ml PBS), stirred, and incubated for 4 hours at 37ºC in a humidified 5% CO2 incubator. The medium was then withdrawn. Following the incubation period, 100 µl of MTT solubilization solution (DMSO, dimethyl sulfoxide, Sigma Aldrich, USA) was added and gently mixed. A microplate reader was then used to measure the absorbance at 540 nm. (Edrees et al., 2017; Faty et al., 2017; Muhammad et al., 2017; Mabkhot et al., 2017; Omha et al., 2017; The OD of the test divided by the OD of the negative control and multiplied by 100 yields the percentage of cell viability. The cytotoxic potential increases with decreasing viability percent value. A sample is deemed cytotoxic if its percentage vitality value is less than 70%; non-cytotoxic if its percentage vitality value is more than 70%

$$\frac{\text{control}-\text{test}}{\text{control}} \times 100$$

III.RESULTS & DISCUSSIONS

1. X-Ray Diffraction Studies

The HAP (A1), HAP-Ag(A2), and HAP-Au(A3) crystal forms were investigated using powder X-ray diffraction analysis (XRD-Bruker, USA). All samples underwent X-ray diffraction (XRD) at voltage and current settings of 35 kV and 30 mA, respectively. Using Cu K radiation, the XRD patterns were recorded in the range of 0 to 100 at a pace of.02 sec /step size. The XRD patterns were crystallographically identified by comparing them to standard data compiled by the International Centre for Diffraction Data (ICDD). Figure 1 shows XRD patterns of pure HAP (A1) that exactly match the specified value of ICDD.

Figure 1 - XRD patterns of Control calcined Hydroxyapatite HAP(A1), HAP-Ag(A2), and HAP –Au (A3) with the reference number from ICDD database number of PDF 01-089-6440.

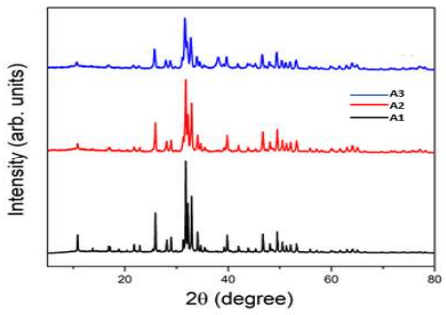

2. Fourier Transformer Infrared Spectroscopy (FTIR)

The creation of HAP by phosphate band symmetry spanning from roughly 1000 to 1100 cm^{-1} was confirmed by the FT-IR patterns displayed in Figure 2. In addition, the peaks with bands at 500 to 650 cm^{-1} belonged to the $PO4^{3-}$ ion.

The FTIR spectra of HAP(A1), HAP-Ag(A2), and HAP-Au(A3) in Figure 2 showed that the hydroxyapatite base structure contains well-dispersed nanoparticles.

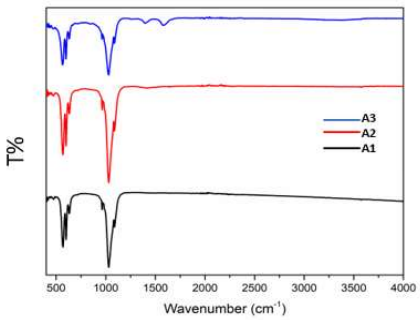

The strong peak among the phosphate vibration modes, the main peaks of the phosphate group were located between 900 and 1100 cm^{-1}(Santos et al., 2008). The broad peak, which represents a stretching vibration of the surface hydroxyl group (OH) as the phases shifted as a result of high-temperature sintering—which may also have been caused by the microwave technique—was not apparent over the 3643 cm^{-1} range. In contrast, bands corresponding to the carbonyl group's (CO^{-}) stretching modes were detected at around 1464 and 874 cm^{-1}. There was also a notable decrease in the carbonyl group at 1400 cm^{-1}, which may have been caused by the Au and Ag groups doping the base compounds' carbonyl groups. The largely well-attended Au and Ag groups' bonding adhesion of Au and Ag groups to a certain degree of gold and silver oxides was observed. Alla S., Tetiana D., et al. (2021) carried out the synthesis and characterization of HAP and composite based on collagen characteristics.

It was previously understood that type A or type B apatite might be produced by carbonate ion replacement at the hydroxyl and phosphate sites in the HAP lattice. It is believed that the HAP preparation is what led to the carbonate ions' presence in the apatite structure. Since the incorporation of nanoparticles was negligible in comparison to the amplified peaks of Ca and PO_4^{3} in the doped spectrums, the FTIR patterns of the HAP, HAP-Ag, and HAP-Au nanoparticles did not show any significant differences in the internal structures. from the pure Hap also validated the well-defined microwave production process since all the spectra match the existing hydroxyapatite and hydroxyapatite doped silver and gold nanoparticles fundamentally.

3. Raman Spectroscopy

The characteristic features of HAP, HAP-Ag, and HAP-Au are displayed in the Raman spectrum (Figure 3). The Raman spectrum displayed an extremely intense band at 963 cm^{-1} that corresponded to the symmetric stretching mode (v1) of phosphate, which is the distinctive peak of HAP (Hickman 2015, Hulbert et al, 1987).

Th: Raman spectra of the heated HAP(A1), Hap-(A2), and Hap-Au(A3) at 1100°C are shown in ure 3.

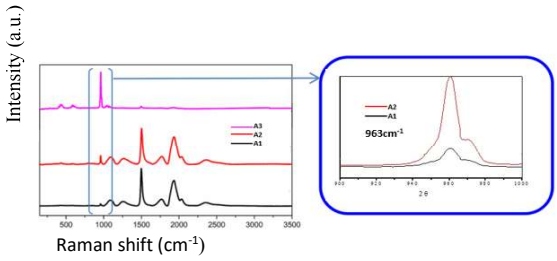

Due to various phosphate group stretching and bending modes, the Raman shift of hydroxyapatite doped with silver and gold nanoparticles is extremely acute, ranging from 50 to 1500 cm^{-1}. The complete symmetric stretching mode of the P-O bond is described by the existence of a very crisp band, especially from 961; in contrast, peaks at 1046 cm1 and 1074 cm^{1} respectively show the triply degenerated asymmetric stretching mode of the identical P-O bond. On the other hand, the double degenerated bending mode of the phosphate group is responsible for the bands located between 480 and 530 cm^{-1}. The O-P-O bonds' vibrations are described by all of the vibrational peaks that have been

mentioned and which characterize the bending modes of the functional group. The peaks' intensities range from 1500 to 3000 is decrease when Au content rises, as shown in the second HAP-Au spectra. The other broad spectrums were decreasing as the silver and gold nanoparticles were trapped in the functional groups of the pure HAP, and the well-defined peaks at 963 cm^{-1} via this spectrum verified the pure form HAP.

4. Scanning Electron Microscopy

Pure HAP sample morphology and elemental composition were analyzed using SEM (SEM). The results are displayed in Figures 4, 5, 6, and 7. The SEM micrographs (Figure 4) showed that the powders' morphology—which forms the flat, awkward flower-type HAP with a particle size of 100 nm—is slightly influenced by the microwave approach. Moreover, the nanoparticles in the SEM pictures tend to aggregate because of their nanometric size. The micrographs show that a decrease in particle size results from an increase in the precise and sharply formed Hap caused by focused microwave treatment carried out in a controlled environment.

Figure 4: SEM images of HAP, HAP-Ag, and HAP-Au, all demonstrated a similar structure the major composition was calcium and phosphate salts of HAP.

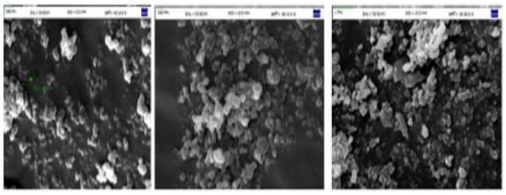

The main components of hydroxyapatite, Ca, Po_4, and O_2, are confirmed by the EDAX spectra. Figure 4 shows how the HAP predominates as a flat, awkward structure, and EDAX analysis assisted in determining the percentage of gold and silver in the hybrid composite to grasp the elemental percentage. Figure 5 only shows Ca and Po_4 as the main elements; there is no evidence of gold or silver. Figure 6 shows less than 3% of gold and no evidence of gold. Figure 7 shows less than 4.5% of silver and no evidence of gold in the powder that was obtained. Additionally examined were the synthesis and physicochemical properties of Ag-doped biomedical applications.

Figure 5: 1. SEM for the pure HAP and it confirms the presence of Ca, P, and O_2.

2. EDAX- no evidence of silver and gold.

1 2

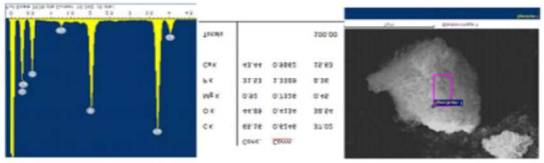

Figure 6: 1.SEM for the pure HAP- Ag and it confirms the presence of Ca, P and Ag.

2.EDAX - less than 4.5% of Ag in the composite.

1 2

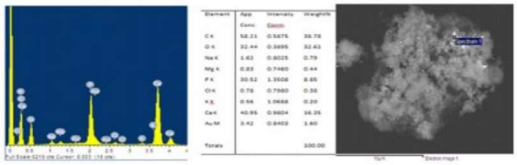

Figure 7: 1. SEM for the pure HAP- Au and it confirms the presence of Ca, P, and Au.

2. EDAX less than 4.5 % of silver in the composites.

1 2

5. Antibacterial activity:

Compounds' antibacterial potential against both gram-positive and gram-negative organisms is clearly shown in Table 1. Compared to all other organisms, Hap-Ag showed the highest level of activity. The pictures of the activity against the organisms are shown in Figure 8. According to Muhammad M. et al. (2021), selenium and strontium co-substituted HAP would increase its antibacterial

activity in vitro against both Gram-positive (Escherichia coli) and Gram-negative (Staphylococcus carnosus) bacteria

Table:1. Antibacterial potential of compounds HAP (A1), HAP- Ag (A2), HAP- Au(A3)

Bacterial Strains	*Zone of Inhibition (mm in Diameter)*				
	A1	*A2*	*A3*	*+Cont.*	*- Cont.*
Staphylococcus aureus (G+)	-	*12*	-	*21*	-
Staphylococcus Mutans (G+)	-	*10*	-	*12*	-
E. coli (G-)	-	*12*	-	*22*	-
Klebsiella pneumoniae (G-)	-	*15*	-	*25*	-

Figure 8: Displayed the images of the activity of A1, A2, and A3 against the bacterial group such as A-S*taphylococcus aureus(G+), B-Streptococcus mutans(G+), and C-E. coli (G-) and D- Klebsiella pneumoniae(G-).*

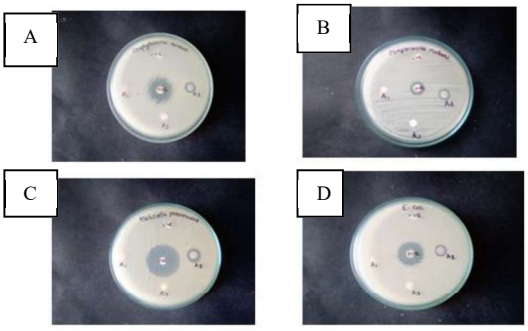

6. Antifungal activity

Table 1 presents the antifungal potential of several compounds against distinct fungal groups. The results did not show statistical significance in

Table 1 presents the antifungal potential of several compounds against distinct fungal groups. The results did not show statistical significance in any of the groups, possibly due to insufficient concentration of the active group, excessive depth of culture development, or a combination of these factors

Table 2. Antifungal potential of compounds -A1, A2 &A3)

Fungal Strains	Zone of Inhibition (mm in Diameter)				
	A1	A2	A3	+ Cont	- Cont
Aspergillus flavus	-	-	-	10	-
Candida albicans	-	-	-	17	-
Aspergillus niger	-	-	-	10	-

Figure 9: Activity of HAP, HAP-Ag, and HAP-Au against the fungal group such as A, *Aspergillus flavus, B, Aspergillus Niger, and C, Candida albicans.*

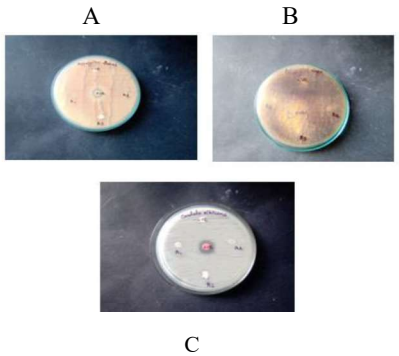

7. Cell cytotoxicity

More than 70% of the cells in all the groups, including HAP, HAP-Ag, and HAP-Au, are viable,

as seen in Figures 10 and 11. It also showed that normal cell growth was unaffected by cell proliferation in three treatment groups. As a result, it was determined that the treatment groups were safe and compatible with the human body.

Figure10: Cell viability of A1, A2, &A3 at different concentrations:

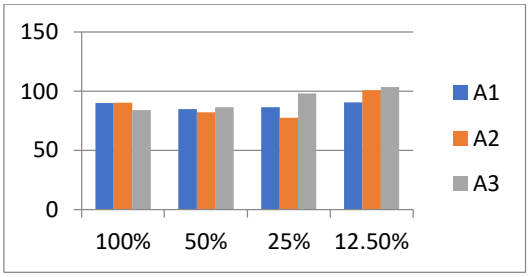

By the end of the second week, the Ca2+deposits in osteogenic differentiation began to accumulate and got denser. The alizarin red treatment gave these deposits a red tint. On day 8, there was a small rise in ALP activity, which peaked on day 14.

Figure 11: Cytotoxicity studies of A1, A2 and A3 at different concentrations

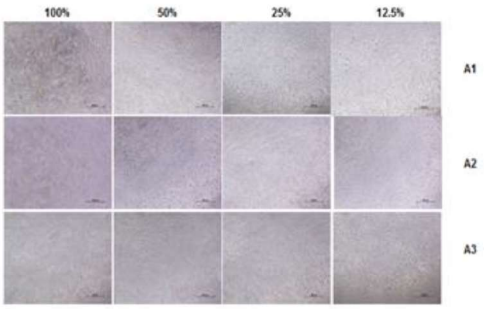

IV.CONCLUSION

A promising option for orthopedic use is the fabrication of HA-doped nanocomposite using advanced microwave assistance. The end product of HA demonstrates a bioactive material that is effective in replacing, reconstructing, and repairing damaged or diseased body parts, particularly the bones. As a result, one possible advancement in the field of orthopedic applications is the synthesis and characterization of HA composites using the strongest microwave apparatus. Because of their osteoconductive qualities and biocompatibility, gold and silver nanoparticles combined with hydroxyapatite form a hybrid composite that has improved bone-bonding capabilities and is frequently utilized in the replacement of hard tissue. When it comes to bond formation, hydroxyapatite outperforms most other bone substitutes, including allografts and metallic implants.

Our current microwave method for creating in-situ gold and silver nanoparticles doped with HAP is offering researchers a great deal of potential because it greatly cuts down on the amount of time needed for synthesis while still meeting repeatability and reproducibility requirements. Overall, the study demonstrates that the synthesis of HAP doped with gold and silver nanoparticles using the microwave approach is both practical and cost-effective when producing large quantities of the material. Meeting the enormous market need for bone cement for a variety of traumatic applications is the intended goal of this research. The current work serves as a preface to the future study, which will assess the various gaps.

ACKNOWLEDGEMENT

The authors would like to express gratitude towards the Department of Biotechnology, Aarupadai Veedu Institute of Technology, for giving consent to carry out the Research Work.

CONFLICT OF INTEREST

The authors disclose no conflict of interest.

REFERENCES

Alla Serhiienko, Tetiana Dotsova, Olena Yanushevska, Andril Lapinsy,& Grigory Krymets..(2022). Synthesis and characterization of hydroxyapatite and composite based on it with collagen. Chem.Paper.Vol 76,Pp.385-392.

Arumugan, S., Rajam A.M., Natarajan, N., Rao, U., Rose, C., and Sastry, T.P. (2006).“Synthesis of silver nanoparticles by surfactant-assisted chemical reduction method” published in the Journal of

Biomedical Nanotechnology. J . Biomed. Nanotechnol. 2, 46 —52 Cross Ref.

Assam, A. J., Dzoyem., J. P., Pieme, C. A., and Penlap, V. B. (2010).In Vitro Antibacterial Activity and Acute Toxicity Studies of Aqueous-Methanol Extract of Sida rhombifolia Linn. (Malvaceae), BMC Complement.Altern.Med.27,10-40.

Bauer, A .W., Kirby, W. M. M., Sherris, J. C & Turck, M. (1966). Antibiotic susceptibility testing by a standardized single disk method. Amer. I. C/in. Pathol. 45:493-496,

Best, S.M., Porter, A.E., Thian, E.S., Huang, J. (2008). Bioceramics, past, present and for the future.J. Eur. Ceram. Soc, 28, 1319–1327.

Correia, R.N., Magalh, M.C.F., Marques, P.A.A.P., Senos, A.M.R. (1996). Wet synthesis and characterization of modified hydroxyapatite powders. J. Mater. Sci. Mater. Med. 7, 501–505.

Dey, A. Bomans,P.H.H., Muller,F.A., Will,J., Frederik,P.M. (2010). The role of prenucleation .clusters in surface-induced calcium phosphate crystallization. Nat. Mater. 9, 1010–1014.

Ding ,Y., Liu , J., Wang ,H., Shen,G., and Yu ,R. (2007). Improved bioabsorbability of synthetic Hydroxyapatite through partial dissolution-precipitation of its surface. Biomaterials, 28, 2147 —2154 CrossRef CAS PubMed.

Dubok, V.A. (2000). Bio ceramics ¾ yesterday, today, tomorrow. Powder Metall. Metal Ceram. 39,7–8.

Gupta, Y., Mathur, G.N., and Verma,S. (2006). synthesis of a new class of compounds and their potential use as inhibitors of a specific enzyme.Bio.org. Med. Chem. Lett.16, 363 —366 CrossRef CAS PubMed.

Hench, L. (1991). Bioceramics, from concept to clinic. J. Am. Ceram. Soc. 74, 1487–1510.

Hickman,K.(2015). Fabrication, Properties and Applications of Dense Hydroxyapatite: A Review.Bioceramics.Ph.D.Thesis,1999. J. Funct. Biomater.1116 -1122.

Hulbert, S.F., Bokros, J.C., Hench, L.L.,Wilson, J., Heimke, G. (1987). Ceramics in Clinical Applications Past, Present and Future; High Tech Ceramics; Elsevier: Amsterdam, The Netherlands, pp. 189–.213.

Kohner ,P.C., Rosenblatt, J.E., & Cockerill, F.R.(1994). Comparison of agar dilution, broth dilution, and disk diffusion testing of Ampicillin against Haemophilus spp. by using in-house and commercially prepared media J. Clin. Micro biol. 321594 –596.

Mathabe M.C., Nikolova R.V., Lall N., Nyazema N. (2006).Antibacterial activities of medicinal plants used for the treatment of diarrhea in Limpopo Province, South Africa, Journal of Ethnopharmacology, 105, pp. 286-293.

Muhammad, M., Qaisar Nawaz., Muhammad Atiq Ur Rahmaan Muhammad Maqbool, Qaisar Nawaz ، M496uhammad Atiq Ur Rehman , Mark Cresswell , Phil Jackson , Katrin Hurle Rainer Detsch, Wolfgang H Goldmann, Asma Tufail Shah , Aldo R Boccaccini,.(2021). Antibacterial activity of Selenium and Strontium substituted hydroxyapatite, Int .j. mol. .Sci. 2021 Apr; 22(8): 4246. doi: 10.3390/ijms22,8,4246,Pp 1-18.

Natarajan, N., Prabasheela,B., and Sujatha Pushpakanth,(2018). Methods for Synthesizing Hydroxyapatite and Doping of Nanoparticles as Biocomposite for Tissue Engineering – A review article, 217, International Journal of Pharmaceutical Research, July- Sept 2018, Vol 10, Issue.3, Pp 213-217.

Nishat Arshi., Faheem Ahmed., Shailendra Kumar., Anwar, M.S., Lu, J., Koo, B.K., Lee, C.G. (2011). Microwave-assisted synthesis of gold nanoparticles and their antibacterial activity against Escherichia coli (E. coli).Curr, Applied. Sci. Vol 11, Issue 1.Pp 5360-5363.

Olszta, M.J., Cheng, X., Jee, S.S., Kumar, R., Kim, Y.Y., Kaufman, M.J., Douglas, E.P., and Gower, L.B. (2007).Bone Structure and Formation; A new perspective. Mater. Sci. Eng., R, 58(3–5), 77–116.

Petit, R. (1999). The use of hydroxyapatite in orthopedic surgery, a ten-year review. Eur. J. Orthop. Surg. Traumatol. 9, 71–74

Ramesh, S. (2001). Grain size—Properties correlation in polycrystalline hydroxyapatite bioceramic .Malays. J. Chem, 3, 35–40.

Ren, F., Xin, R., Ge, X., and Leng, Y. (2009). Characterization and structural analysis of zinc-substituted hydroxyapatites," Acta Biomaterialia, vol. 5, no. 8, pp. 3141–3149.

Santos, M.H., Dias Heneine, L.G., and Mansur, H.S. (2008). Synthesis and characterization of calcium phosphate/collagen bio composites doped with Zn2+, Materials Science and Engineering C, vol. 28, no. 4, pp. 563–571.

Sebastiammal S. Fatima Arul sigamani, Saud Alarifi, Shahid Mahboob , Johnson Henry , M.R. K avipriya , Marimuthu Govindarajan , Marcello Nico letti , Vaseeharan.B (2022).Synthesis and Physicochemical characterization of Ag-doped Hydroxyapatite nanoparticles and their potential biomedical applications. Vol;210,112979. Pp.215-223.

Sikder M Asaduzzaman,Masud Rana,Naznin Akhtar Sheifur Rahman.Extraction of Hydroxyapatite from Bovine and Human Cortical Bone by Thermal Decomposition and Effect of Gamma Radiation: A Comparative Study. International Journal of Complementary & Alternative Medicine, vol.10; Issue;3, Pp 1-10.

Sinha, A., Mishra, T., Ravishankar, N. (2009). Polymer-assisted hydroxyapatite microspheres suitable for biomedical application. J. Mater. Sci. Mater. Med. 19.Pp2009-2013.

StructureofBoneTissueAvailableOnline:.http://training.seer.cancer.gov/anatomy/skeletal/tissue.html (accessed on 10 December 2015).

Suganya P. K. Elayaraja , M.I. Ahymah Joshy , V. Sarath Chandra · E.K. Girija, (2017). Biopolymer Zein-coated gold nanoparticle: synthesis antibacterial potential. J. Photo chem. photobiol. B.Biol. Vol.31, Issue.3, Pp593-599.

Tang, Y., Chappell, H.F., Dove, M.M., Reeder ,R.J and Lee, Y.J. (2009). Zinc incorporation into hydroxyapatite," Biomaterials, vol. 30, no. 15, pp. 2864–2872.

Turkoz M. Aykan Onur Atilla, and Zafer Afis .(2017).Silver and Flouride doped Hydroxyapatite .Ceram.Int. Vol; 39,Issue.8, Pp.8925-8931.